

1971

The kinetics of manganese oxide reduction from blast furnace-type slags by carbon-saturated iron

Charles Kendall Clarke

Lehigh University

Follow this and additional works at: <https://preserve.lehigh.edu/etd>



Part of the [Materials Science and Engineering Commons](#)

Recommended Citation

Clarke, Charles Kendall, "The kinetics of manganese oxide reduction from blast furnace-type slags by carbon-saturated iron" (1971). *Theses and Dissertations*. 3888.

<https://preserve.lehigh.edu/etd/3888>

This Thesis is brought to you for free and open access by Lehigh Preserve. It has been accepted for inclusion in Theses and Dissertations by an authorized administrator of Lehigh Preserve. For more information, please contact preserve@lehigh.edu.

THE KINETICS OF MANGANESE OXIDE REDUCTION FROM BLAST
FURNACE-TYPE SLAGS BY CARBON-SATURATED IRON

Charles Kendall Clarke

1

ABSTRACT

The reduction of MnO from a slag containing $\text{CaO}:\text{SiO}_2:\text{Al}_2\text{O}_3$: 5:4:1, in those weight proportions, by carbon-saturated iron was studied to determine the rate controlling mechanism of the reaction. An initial true reaction order of 1.77 was determined by differential methods using data from all four runs. Each separate run was found to fit second-order reversible kinetics for the first four to eight minutes by integral analysis. Time orders of 3.05 to 4.06 were found after the first ten minutes of the reaction and these orders appeared to vary with the initial MnO concentration. From this information, the reaction was divided into two stages. The first stage of the reaction was initially chemically controlled for the first few minutes of the reaction and then the reaction entered a transition region. The second stage of the reaction was marked by the appearance of a linear relation in the differential time data and was transport controlled.

**THE KINETICS OF MANGANESE OXIDE REDUCTION FROM BLAST
FURNACE-TYPE SLAGS BY CARBON-SATURATED IRON**

by

Charles Kendall Clarke

A Thesis

Presented to the Graduate Committee

of Lehigh University

in candidacy for the Degree of

Master of Science

in

Metallurgy and Materials Science

Lehigh University

CERTIFICATE OF APPROVAL

This thesis is accepted and approved in partial fulfillment of the requirements for the degree of Master of Science.

January 5, 1971
(Date)

Stephen K. Farby
Professor in Charge

A. P. Canard
Head of the Department

ACKNOWLEDGEMENTS

I would like to extend my appreciation to all those who have helped in the preparation of this thesis. I am especially indebted to the following:

To Dr. S. K. Tarby, my thesis advisor, for his encouragement and advice,

to F. H. Ruch and his laboratory technicians for assisting me in analyzing the slag and iron samples,

to W. Mohylsky and his shop crew for fabricating experimental equipment,

to B. Hayes for typing the thesis,

to the Chemical Metallurgy program and the companies listed below for their support of my graduate studies and this research project:

American Metal Climax Corporation,

Bethlehem Steel Corporation,

Carpenter Technology Corporation,

St. Joe Minerals Corporation,

The New Jersey Zinc Company and

United States Steel Corporation, and

to my wife Carolyn who has helped with the chemical analysis and typing of this thesis.

TABLE OF CONTENTS

	Page
Title Page -----	i
Certificate of Approval -----	ii
Acknowledgements -----	iii
Table of Contents -----	iv
List of Tables -----	v
List of Figures -----	vi
Nomenclature -----	vii
Abstract -----	1
Introduction -----	2
Experimental Procedure -----	9
Results -----	14
Discussion -----	28
Conclusions -----	31
Tables -----	32
Appendix -----	41
References -----	54
Vita -----	55

LIST OF TABLES

Table	Title	Page
I	Materials Used in Project -----	32
II	Experimental Data Slag Analysis -----	33
III	Integral Second Order Data -----	37
IV	Time Orders of the Experimental Runs -----	39
V	Comparison of Fluxes Predicted by Szekely's Model with the Observed Fluxes -----	40

LIST OF FIGURES

Figure	Title	Page
1	Schematic Drawing of the Furnace -----	10
2	Crucible Details -----	11
3	Plot of Experimental Data at 1500°C and 1 atm CO Gas -----	15
4	Reversible Second-Order Data for Run 2 -----	16
5	Reversible Second-Order Data for Run 3 -----	17
6	Reversible Second-Order Data for Run 4 -----	18
7	Reversible Second-Order Data for Run 5 -----	19
8	Data Taken from all Four Runs Produced a True Differential Reaction Order of 1.77. -----	21
9	The Differential Time Order for Run 2 Was Found to be 3.88. -----	22
10	The Differential Time Order for Run 3 Was Found to be 3.72. -----	23
11	The Differential Time Order for Run 4 Was Found to be 4.06. -----	24
12	The Differential Time Order for Run 5 Was Found to be 3.05. -----	25

NOMENCLATURE

- C_A - Concentration of A in moles/cm³
- C_{A_0} - Initial concentration of A in moles/cm³
- C_{A_e} - Equilibrium concentration of A in moles/cm³
- \bar{C}_i - Bulk concentration of species i in moles/cm³
- D_A - Diffusivity of species A in cm²/min
- k - Reaction rate constant in (cm³)ⁿ⁻¹/min·molesⁿ⁻¹, where n is the reaction order
- K_c - Equilibrium constant
- \bar{N}_{MnO} - Average molar flux of MnO in moles/cm²·min
- S - Interfacial area in cm²
- t - Time in minutes
- t_e - Time between rising bubbles
- V - Volume in cm³
- X_{MnO} - Fraction of MnO reduced
- Z - Distance from the slag-metal interface in cm

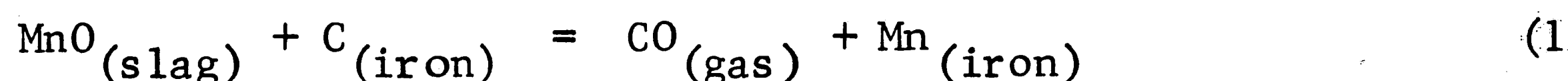
ABSTRACT

The reduction of MnO from a slag containing $\text{CaO}:\text{SiO}_2:\text{Al}_2\text{O}_3:$ 5:4:1, in those weight proportions, by carbon-saturated iron was studied to determine the rate controlling mechanism of the reaction. An initial true reaction order of 1.77 was determined by differential methods using data from all four runs. Each separate run was found to fit second-order reversible kinetics for the first four to eight minutes by integral analysis. Time orders of 3.05 to 4.06 were found after the first ten minutes of the reaction and these orders appeared to vary with the initial MnO concentration. From this information, the reaction was divided into two stages. The first stage of the reaction was initially chemically controlled for the first few minutes of the reaction and then the reaction entered a transition region. The second stage of the reaction was marked by the appearance of a linear relation in the differential time data and was transport controlled.

INTRODUCTION

The kinetics of slag-metal reactions had not been studied in any great detail until the last ten years. Up until this time, most work was spent on determining steady-state requirements or the thermodynamics of reaction systems. The advent of new technology such as vacuum degassing and Basic Oxygen Furnaces has placed a large emphasis on reaction kinetics. The computer is also placing new emphasis on kinetics via process control. Many industrial processes such as the iron-making blast furnace are now being modeled mathematically on computers and any attempt to go beyond an equilibrium model into a dynamic model must consider reaction kinetics. The kinetic aspects of a reaction can also qualitatively give the direction to proceed in constructing a mathematical model or designing a reactor for the process.

This work studied the kinetics of reduction of MnO from a blast furnace-type slag by carbon dissolved in iron. The chemical equation for the reaction is given by Eq. 1.



This reaction occurs in the hearth region of the blast furnace where carbon is the principal reducing agent. Consideration should be given this reaction in any blast furnace model since the manganese content of the iron product is frequently important in future uses of the iron.

It should be noted that this reduction reaction involves the evolution of CO gas which more will be said about later.

In looking at heterogeneous reaction kinetics, the reaction system under study should first be examined qualitatively. One of the first things to be determined is the physical contacting pattern which will determine whether or not the fluid dynamics of the system must be considered. It must also be known if the reaction proceeds by several

steps and whether these steps occur in parallel or series.

Slag-metal systems in which the slag forms as an immiscible layer over a molten metal layer can be described as proceeding in three basic steps which occur in series. Therefore, any one step appreciably slower than the rest will control the reaction rate. 1) The reactants must come to the slag-metal interface by either convective or diffusive transport. 2) An interfacial reaction must occur which may also be broken down into steps as will be described later. 3) The products must then be removed from the interface by convective or diffusive transport.

At the high temperatures involved in iron-making (around 1500°C), there are good reasons to believe that the rates of the chemical reactions are infinitely fast compared to other possible controlling steps.¹ If this were the case, then transport of reactants and products would be the likely rate-controlling aspect of the reaction. The chemical reaction may still be the rate-controlling process in a reaction system involving gas evolution if the rate of agitation of the slag and/or metal were high enough. The stirring would eliminate transport as a factor in the reaction. So a third possibility arises in that as the rate of the reaction subsides, the rate-controlling mechanism may shift from that of reaction control to transport control producing a transition region in which there is no overriding controlling mechanism.

The MnO reduction reaction first studied by Tarby and Philbrook² is a relatively fast reaction involving considerable gas evolution. It was found, as did later work by Koncsics,³ that the reaction could be divided into two parts with different orders of reaction. This type of behavior was also noted in similar studies of the reduction of FeO from slags by carbon-saturated iron.^{2,4} Therefore, these reactions may have undergone a transition from chemical reaction control to transport control. Various models describing these two mechanisms will now be discussed.

Reaction Control

Most kinetic studies usually begin by trying to find some relation between the species of interest and the reaction rate. For a reaction such as given by Eq. 2, this is usually attempted by considering an expression in the form of Eq. 3. The sum of the exponents of the concentration terms is the total order of the reaction or the reaction may be said to be x order with respect to species A.



$$\text{rate} = -kC_A^x C_B^y C_C^z \dots \quad (3)$$

That this procedure is usually followed in trying to find a chemical reaction control mechanism does not imply that reaction orders specify chemical control. A diffusion controlled reaction can show first order kinetics. Integral orders of reaction (0,1,2, etc.) do offer some clues to the reaction mechanism if it is simple.

The order of a reaction such as that given by Eq. 4 may be found by integrating the rate equation (Eq. 5) to obtain an expression as a function of time (Eq. 6). If the data are plotted as the left-hand side of Eq. 6 vs. time and they fall on a straight line, the reaction may then be said to be first order for this case.



$$\frac{1}{V} \frac{dn_A}{dt} = \frac{dC_A}{dt} = -KC_A \quad (\text{constant volume}) \quad (5)$$

$$\ln \left(\frac{C_A}{C_{A_0}} \right) = -kt \quad (6)$$

A more general method for determining reaction orders and the one most fraught with error is the differential method.⁵ Two different

reaction orders may be determined in this analysis, a true reaction order and a time reaction order. In this method, the logarithm of Eq. 3 is taken as follows:

$$\ln (-\text{rate}) = \ln(k) + x \ln(C_A) + y \ln(C_B) + z \ln(C_C) + \dots \quad (7)$$

The instantaneous initial reaction order or the true order is found by measuring the initial slopes of several concentration vs. time curves (for different starting compositions) and the initial compositions. Equation 7 can then be solved for the true orders of each species by a regression-type analysis. The time order is found in the same manner except that slopes and concentrations from one concentration vs. time curve are used. Any difference between the two orders is significant. A true reaction order lower than the time order is an indication of the products of the reaction interfering with and retarding the reaction rate. The reverse case occurs with an autocatalytic reaction.

The reaction orders determined do not indicate chemical or transport control specifically so other means must be used to determine which case is important. One method which has been widely used to provide a qualitative answer is to vary the slag stirring rates and the reaction temperature. The effect of stirring the slag should be small on a chemically-controlled reaction (provided that the surface area is not changed), whereas a transport-controlled reaction would be speeded up with increased stirring due to a decrease in the effective diffusion path. Varying the reaction temperature is not quite so obvious. Diffusion-controlled reactions are assumed to have lower activation energies than chemically-controlled reactions and hence, have a smaller temperature dependency.¹ However, since neither of these energies are usually known unambiguously, this argument is not very strong. A better means of establishing chemical control would be to hypothesize a reaction model and then test it.⁶

The chemical reaction model currently in vogue is adsorption for gas-solid and liquid-liquid reactions. Adsorption is the concentration of some species in the surface of a phase. In the case of slag-metal systems, the dissociated species in the slag are assumed to combine into their molecular forms on the slag surface at the slag-metal interface. The species then react with the other reactants dissolved in the iron phase while at these sites. The reaction products must then desorb from the slag surface sites and diffuse back into their respective bulk phases. There is some evidence of this phenomenon in the literature⁷ regarding molten FeO; however, additional independent data regarding adsorption are needed to verify the model. Because there were no such data in the literature for the system under study, no attempt was made to use this model.

Transport Control

There are two methods currently in use for describing transport control. One is the boundary layer theory and the other is the surface renewal theory. The boundary layer theory assumes that there is a laminar flow boundary layer at the slag-metal interface and turbulent fluid beyond. Calculations of the reaction rate are based on diffusion through this laminar boundary layer as the rate-controlling step. However, this boundary layer is not capable of direct measurement and there is little proof of its existence.^{8,9} Another fault of the boundary layer is that it is not capable of predicting the course of a reaction a priori. The boundary layer thickness determined experimentally is useful only under those conditions in which it was measured. Therefore, this approach yields little in the way of understanding the mechanism of a reaction. The approach is useful in plant operations where an empirical relation of the form:

$$\text{rate} = \frac{D_A}{\delta} (C_A - C_{A_e}) = h (C_A - C_{A_e}) \quad (8)$$

may be used with the measured mass transfer coefficient, h .

The surface renewal approach is possibly more consistent with the physical situation.⁸ This approach pictures a turbulent fluid which continually brings small slugs of fresh fluid to the reaction interface where laminar flow prevails and the species diffuse to the interface. After some variable resident time, the slugs return to the bulk fluid to be remixed. Unfortunately, the distribution of surface residence times must be determined experimentally for each case. Tarby and Philbrook found qualitative agreement of their data with this model though the distribution of surface residence times was not known. Because the model is in part based on the empirical surface residence time function, it is of little use in determining the mechanism of the reaction or for predicting reaction rates for new and different conditions.

Szekely has proposed a more realistic mathematical model for a bubble stirred slag-metal system based on the assumption that at iron-making temperatures all reactions are infinitely fast and mass transfer of reactants and products is the rate-limiting step in the reaction process. In deriving his model, a slag-metal system was pictured in which the steady state concentration profiles of both reactants and products were established. A bubble rising from the bottom of the metal bath then completely disrupted the concentration profiles in both the iron and the slag to the extent that there were no gradients left in the vicinity of the path of the bubble. These concentration gradients were re-established by unsteady state diffusion. By averaging the instantaneous, unsteady state flux over the time period between successive rising bubbles, Szekely was able to compute an average flux for such a bubble stirred system. Assumptions made to use an analytical solution to Fick's Second Law restrict the applicability of the solution to the situation in which the bulk concentrations change little with time (semi-infinite medium) and the diffusivities are relatively constant. (The derivation of the appropriate equations for the system

under study are shown in Appendix I.) This is the mass transfer model which will be used in this study since it was the closest to reality.

In conclusion, it should be restated that kinetic research is important since it gives us an understanding of how important reactions proceed. The very first efforts are usually directed towards determining some expression, empirical or otherwise, for the reaction rate. This is done to provide mathematical models for industrial processes. Next the reaction mechanism should be determined to shed more light on the process and enable us to improve any commercial processes. The problem in heterogeneous kinetics is to determine whether the reaction is chemically controlled, or transport controlled, or a combination of both. This is the problem to which this paper will now address itself.

EXPERIMENTAL PROCEDURE

Apparatus

The experiments were carried out using a 10,000 cycle, 30KVA Ajax Magnethermic induction furnace. Figure 1 describes the actual furnace details. A fused silica cylinder was placed inside the induction coils which were housed in a transite box. This cylinder served to contain the CO gas which was used as the furnace atmosphere. A water-cooled brass top served to seal the cylinder and contained fixtures for the gas lines and the stopper rod assembly. The stopper pull rod came up through the main sampling hole and was sealed with a rubber stopper and held in place with springs as shown.

Spectrographic grade graphite was used in making the crucible assembly and stopper rod. Using two separate crucibles (Fig. 2) allowed the slag to be melted separately from the iron and, since both slag and iron were molten at the start of the experiment, an initial starting time could be unambiguously determined. Vent holes were placed in the metal crucible to prevent an explosion in case the stopper rod leaked.

One atmosphere of carbon monoxide gas purified with Ascarite and Drierite was maintained in the furnace. This was done to keep the activity of the gas at unity for the reaction. A side benefit of this atmosphere was that the slag crucible and stopper rod could be repeatedly used since they were not attacked by the atmosphere or the slag.

Temperatures were recorded with a platinum - 6% rhodium/platinum-30% rhodium thermocouple inserted into the base of the crucible and connected to a recorder. The thermocouple and recorder were compared against a calibrated thermocouple and found to be about 5.6°C too high at 1500°C. Temperature of the furnace was manually controlled and held at 1500°C, within $\pm 5^\circ\text{C}$.

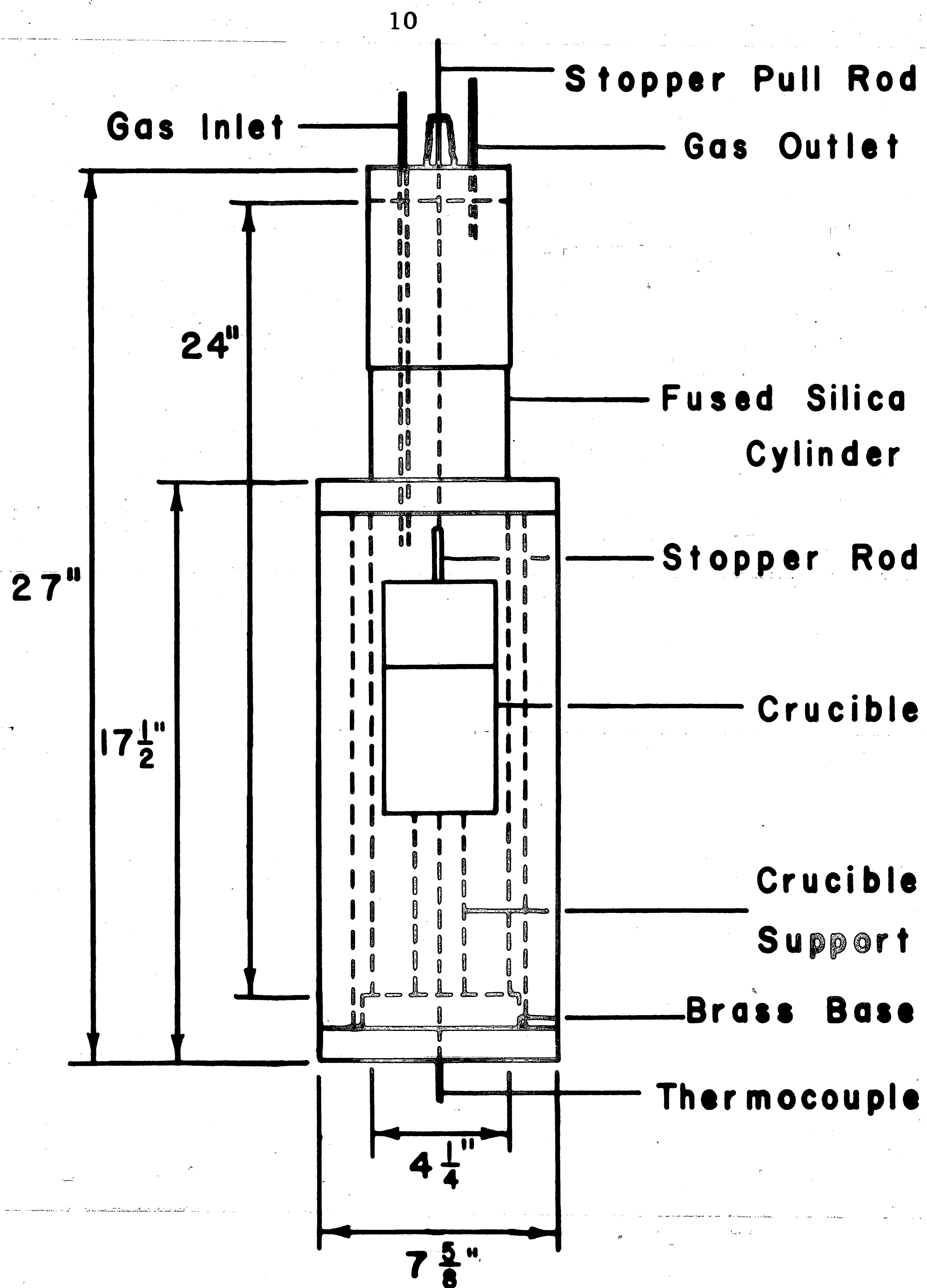


FIGURE 1: Schematic Drawing of the Furnace

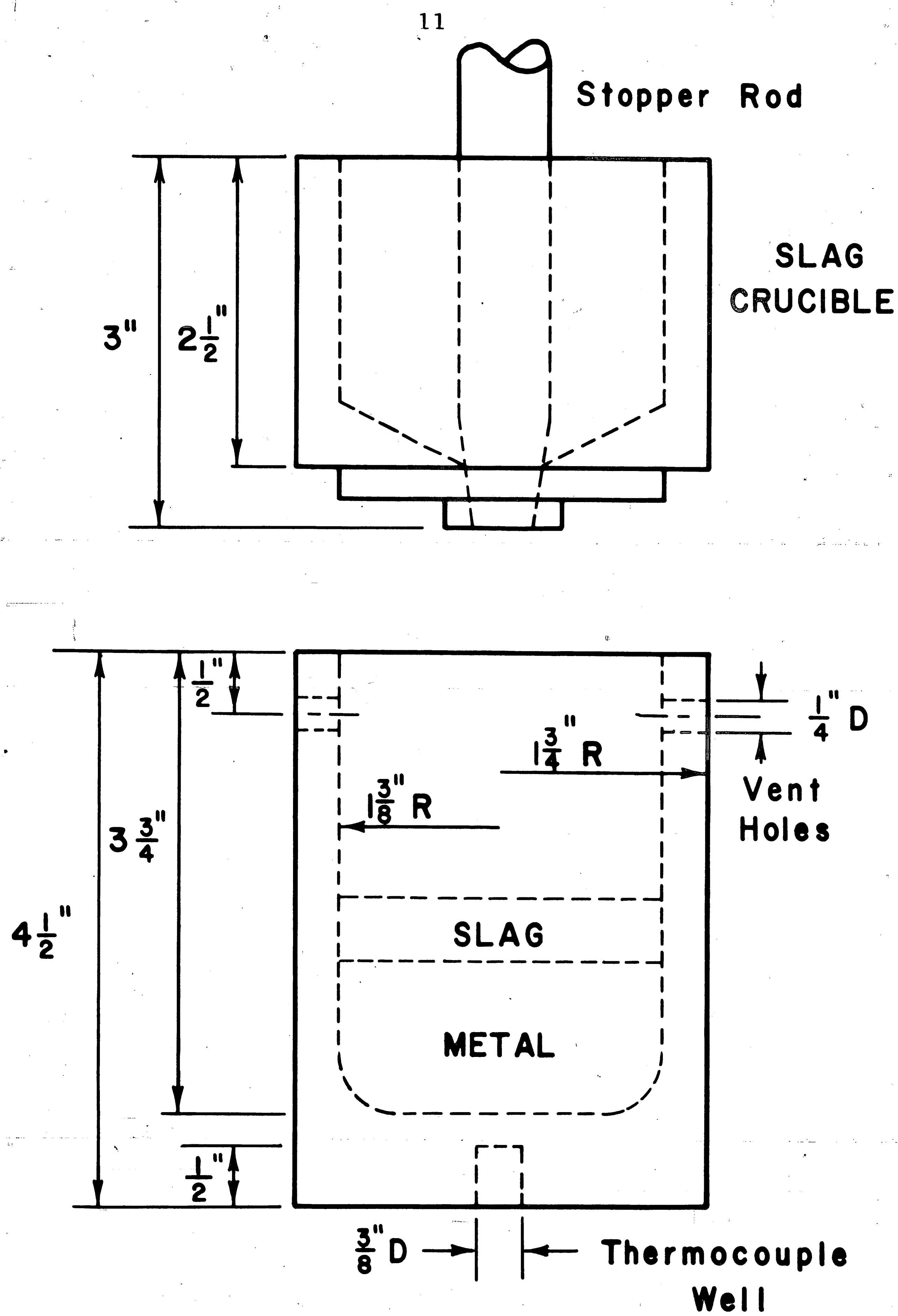


FIGURE 2: Crucible Details

Operating Procedure

The slag components were weighed out to give on a weight basis the following ratio: $\text{CaO} : \text{SiO}_2 : \text{Al}_2\text{O}_3 : : 5 : 4 : 1$. (A complete listing of all materials used is given in Table I.) The slag components were then mixed dry with the appropriate MnO addition (the MnO_2 charged was assumed to go rapidly to MnO at $1500^\circ\text{C}^{2,3}$). A total of 151.0 g slag (in final form, i. e. CaO and MnO) and 600.0 g carbon-saturated iron were charged into their respective crucibles prior to each run. The stopper rod was sealed with a small amount of refractory cement and the slag charge rammed into its crucible to insure melting.

At the beginning of the run, the two crucibles were pinned together with molybdenum pins and placed into the furnace. The CO gas was turned on and the furnace rapidly heated to above 1500°C to melt the slag and then stabilized at 1500°C for 5-10 minutes. A sample of the slag was taken by immersing a 1/4"-diameter copper chill rod into the slag and withdrawing approximately one gram of slag. The stopper rod was pulled after sampling and a clock simultaneously activated to start the run. Sampling was continued in the same manner for around one hour and approximately 10-15% of the initial slag charge was removed during sampling. An iron sample was taken at the end of the run with a quartz tube syringe. A CO gas flow rate sufficient to flush the gas chamber once per minute was maintained during the run.

Chemical Analysis

The persulfate method was used to analyze for manganese in the slag samples.¹² (A complete description of the analysis is shown in Appendix II.) Slag samples were first crushed to -100 mesh in a porcelain mortar and pestle and magnetically cleaned. The entire sample was then weighed into a beaker and dissolved in HCl acid. After the sample had completely dissolved, H_2SO_4 acid was added and the beaker

contents were fumed hard twice. The samples were then brought to volume and the CaSO_4 precipitate allowed to settle out. Samples were then aliquotted into erlynmeyer flasks and mixed acids along with AgNO_3 were added. After cooling to room temperature, the samples were titrated with a sodium arsenite solution standardized against a slag of known Mn content (British Standards 174/1 B.S.). In most cases, at least three titrations were made for each sample.

Samples of iron taken at the end of the experiment and slag samples for ferrous iron analysis were analyzed by the chemical analysis branch at the Homer Research Laboratories of the Bethlehem Steel Corporation.

RESULTS

Data

Four experimental runs were made at 1500°C, $\pm 5^\circ\text{C}$ and one atmosphere carbon monoxide gas. The data are given in Table II and are shown in Figure 3. The smooth curves in Figure 3 were arbitrarily drawn with French curves. FeO analysis was spot checked in two runs (2 and 3) and these few values indicate that some side reaction with the iron did occur. No FeO was initially present in the slag. There was some difficulty in making a mass balance at the end of the reaction as the iron samples showed more manganese than was initially charged.

Reaction Orders

First- and second-order integral reaction order expressions were used first on the data with no conclusive results reached. (See Appendix III for derivation of equations.) However, upon dropping the initial concentration data point and using the first data point after starting the reaction, the data fit both expressions for the first four to eight minutes of the reaction. The results for the second-order expression (Eq. 9) are shown in Table III and

$$\ln \frac{X_e - (2X_e - 1) X}{X_e - X} = \frac{2k_1}{K} C_{\text{MnO}} \cdot t \quad (9)$$

Figures 4-7. It was difficult to ascertain from the rate constants whether first- or second-order kinetics were the appropriate case. The rate constants varied roughly the same amount in both cases. The choice of second-order kinetics was based on the true reaction order which will be discussed later. It should be said that, in all cases, the carbon and CO concentrations were assumed constant.

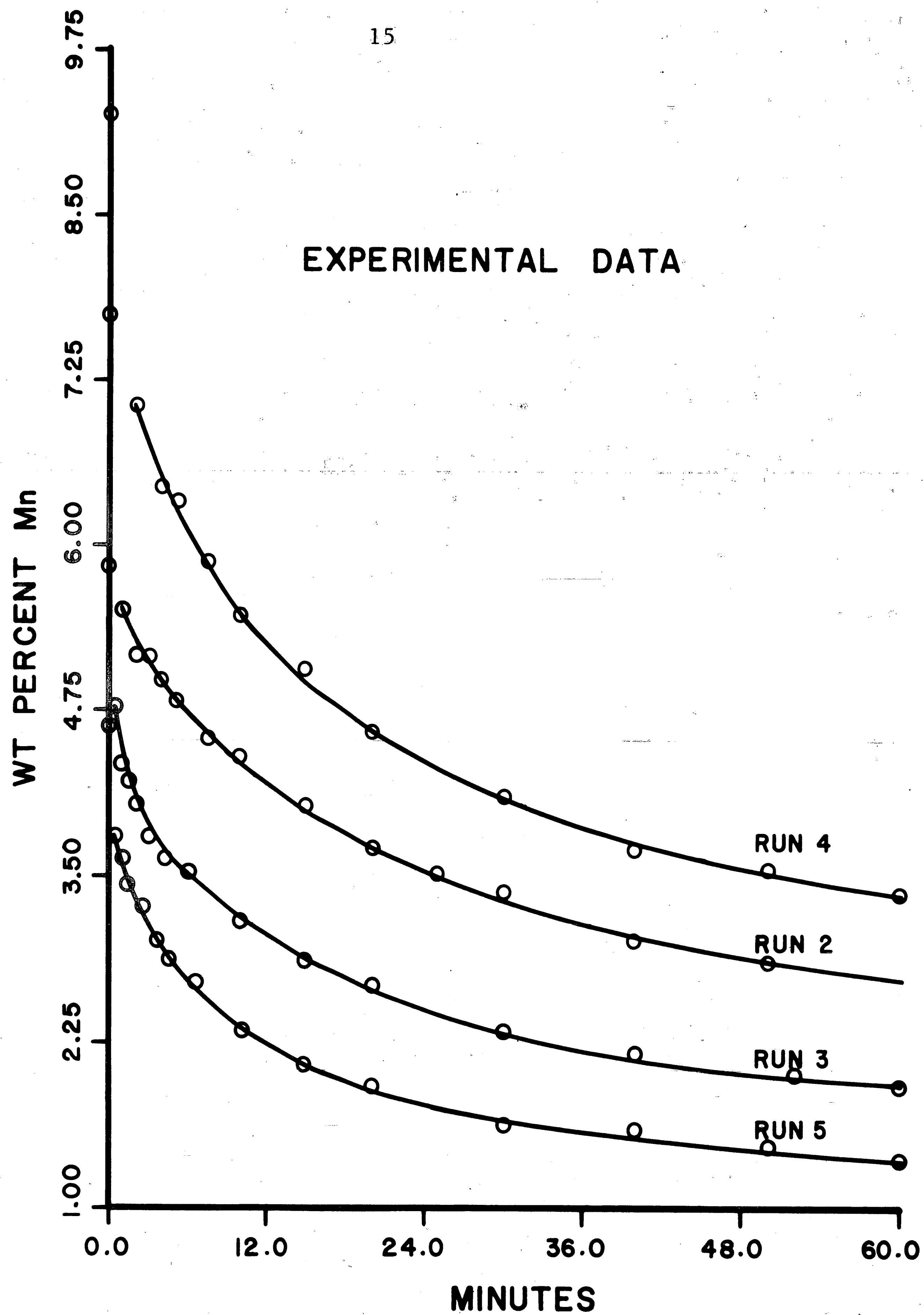


FIGURE 3: Plot of Experimental Data at 1500°C and 1 atm CO Gas

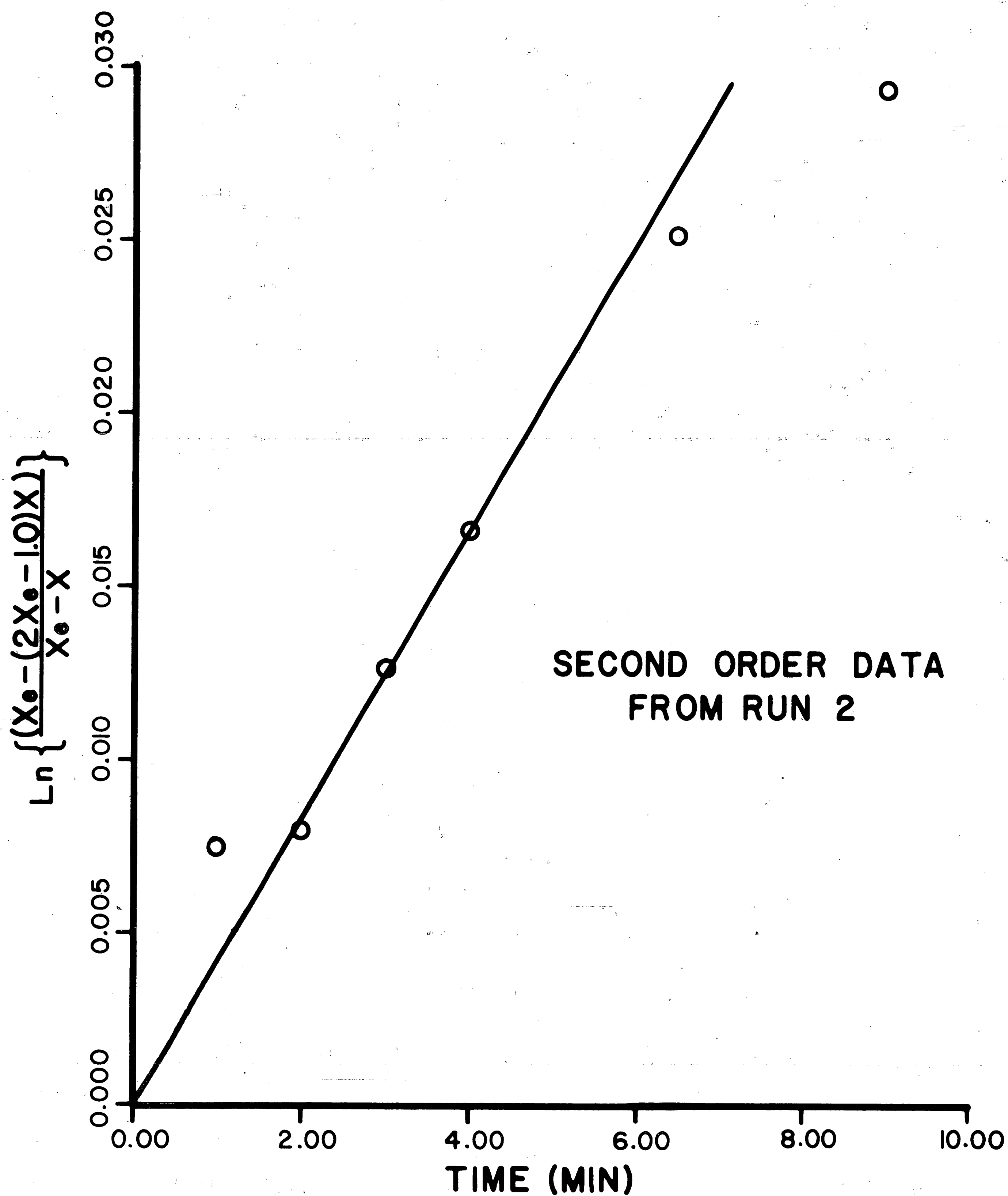


FIGURE 4: Reversible Second-Order Data for Run 2

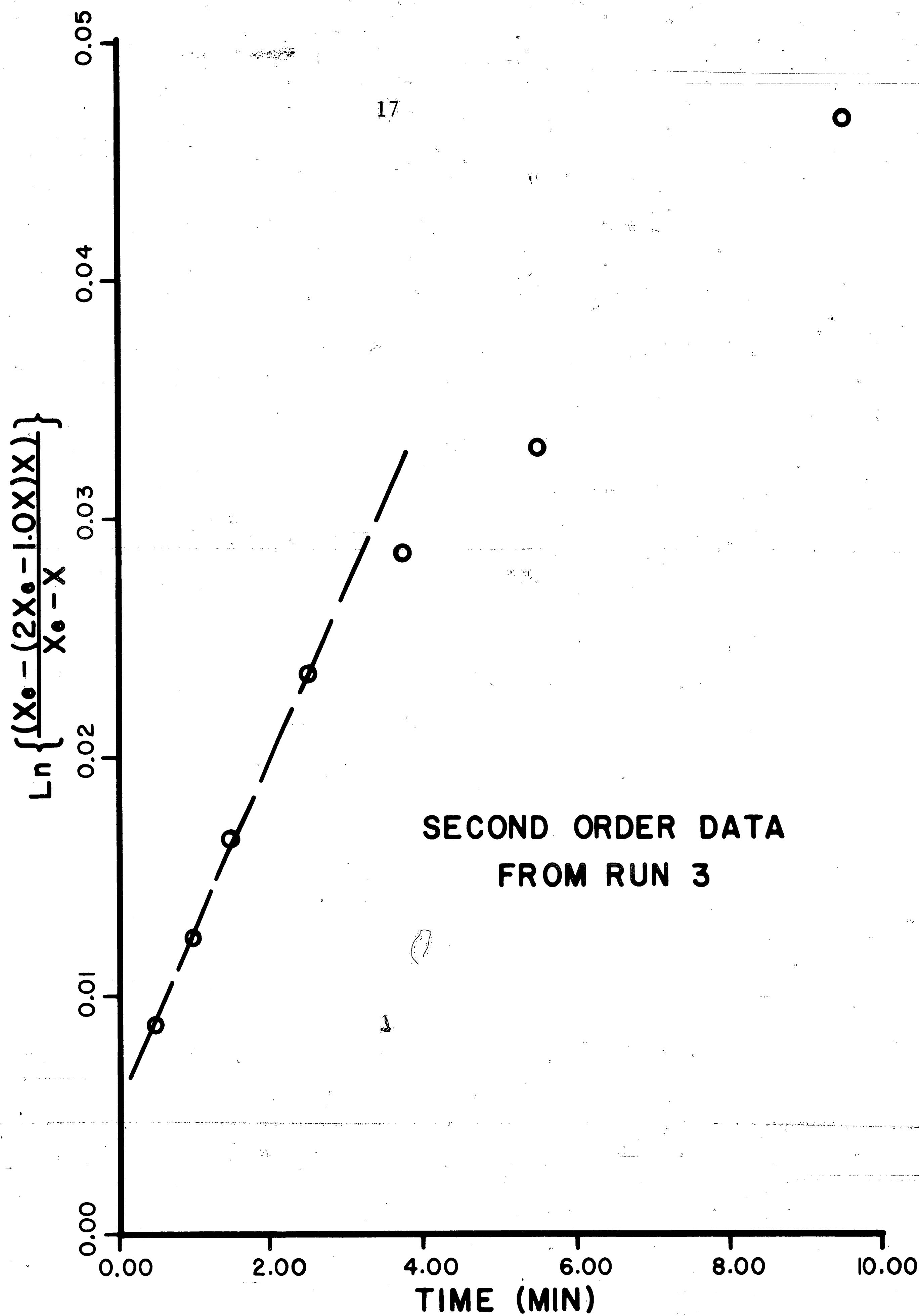


FIGURE 5: Reversible Second-Order Data for Run 3

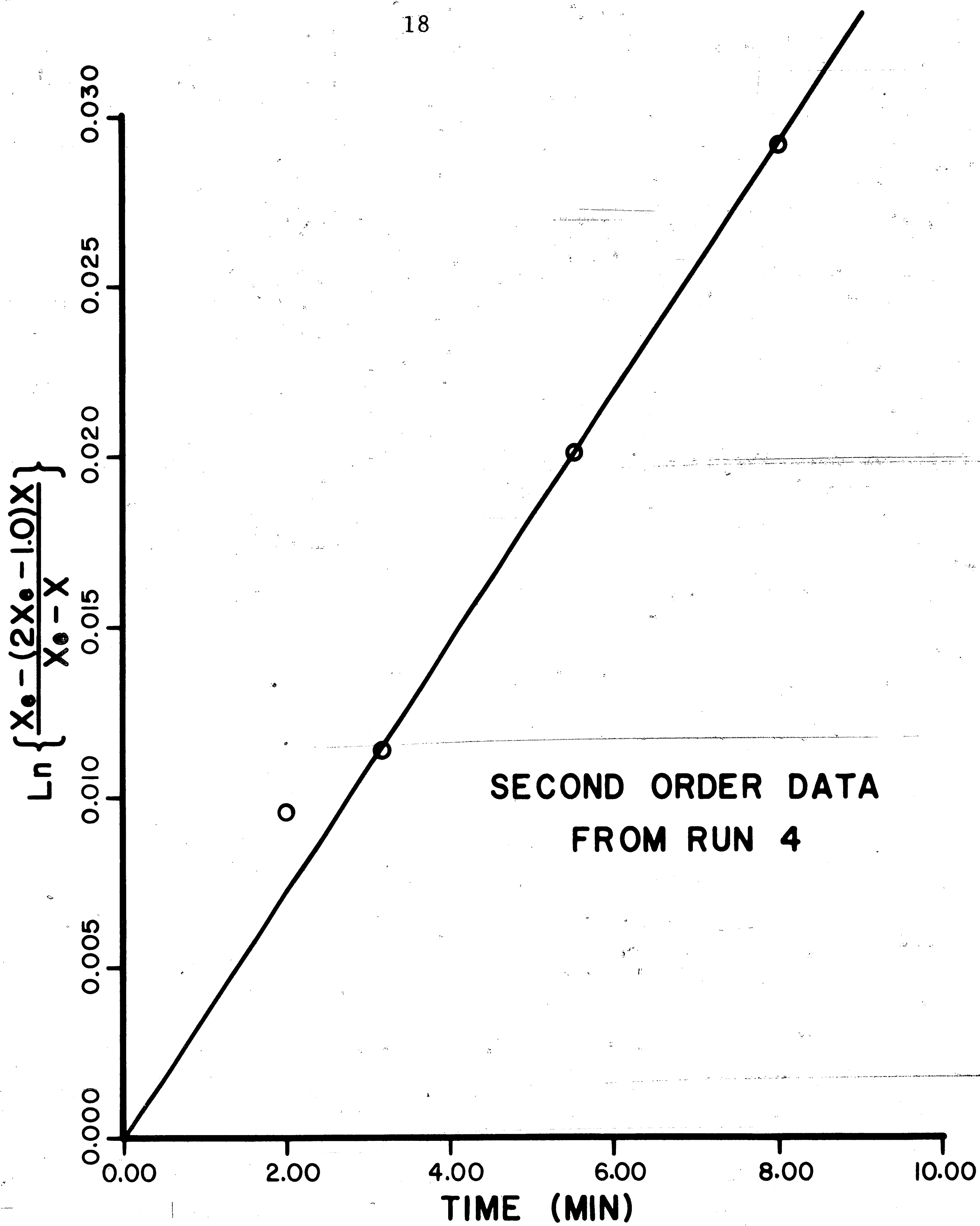


FIGURE 6: Reversible Second-Order Data for Run 4

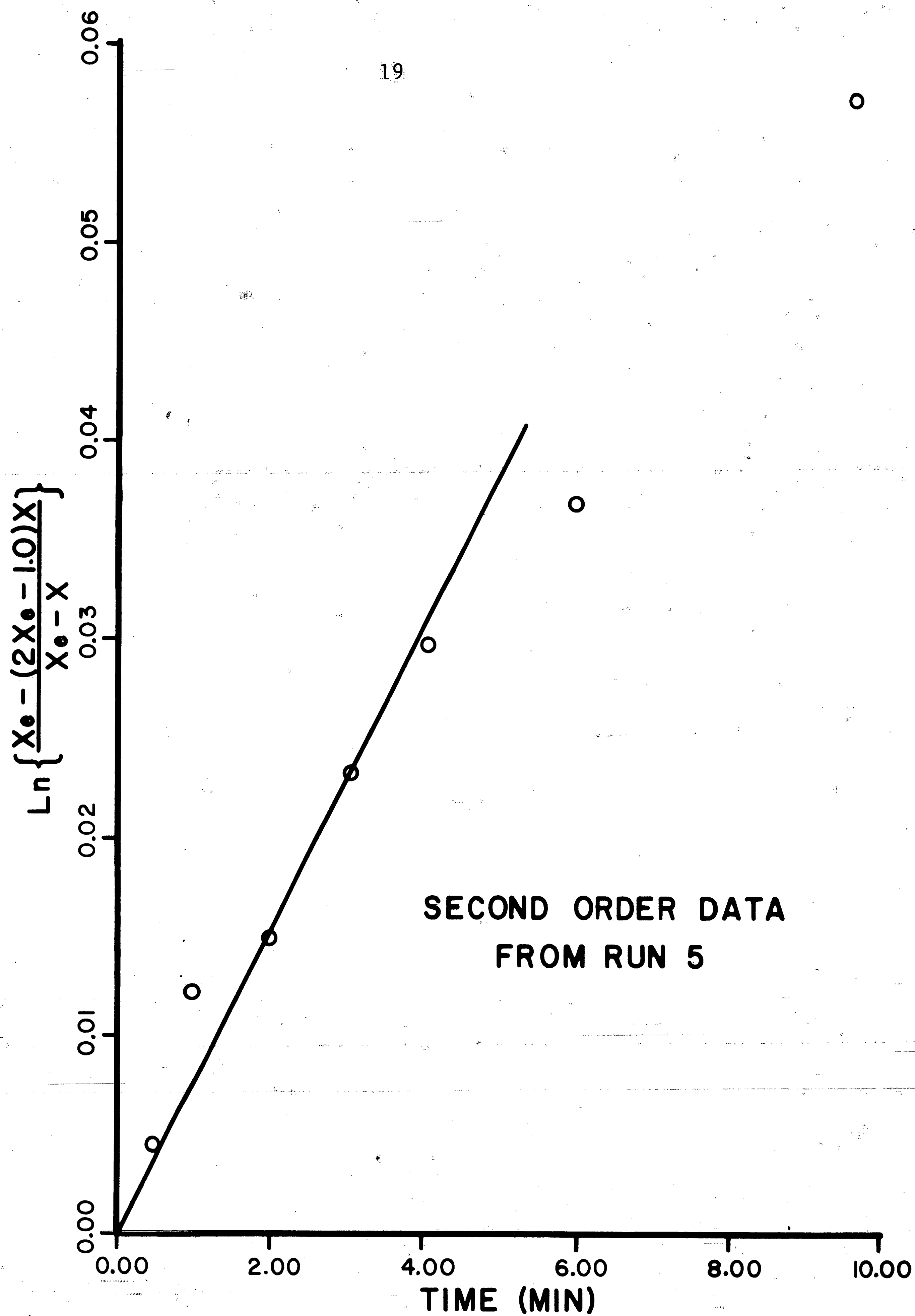


FIGURE 7: Reversible Second-Order Data for Run 5

The method of starting the reaction was probably responsible for the initial concentration data appearing inconsistent with the rest of the data. Slag was dropped onto the metal to start the reaction and there was probably a large slag-metal interfacial area present for a short time. This would result in an abnormally high reaction rate regardless of the reaction mechanism. Therefore, the dropping of the initial concentration data was justifiable.

The initial data were retained in determining a true differential reaction order of 1.77 from the initial slopes of the concentration vs. time data (Fig. 8). A constant carbon concentration made it possible to use the slope of the curve in Figure 8 as the reaction order (Appendix IV). When the large amount of error involved in determining the initial slopes is considered, there is probably not much difference between using the initial data points or the second data points. The true order determination must be made at the very beginning of the reaction before the products of the reaction can interfere. The integral second-order data and the true order of 1.77 also support each other.

The data in each of the four runs were analyzed for their respective differential time orders. Linear portions of the curves (Fig. 9-12) whose slopes corresponded to the order could be found, but the slopes for the different runs were not the same. The time order varied directly with the initial MnO content in the slag (except for Run 3) as shown in Table IV. These linear portions of the differential data which seem to delineate a second stage of the reaction all start at around the same reaction rate as shown by the dashed lines in Figures 9-12. A comparison of the true and time orders shows that the reaction rate is falling off faster than predicted and thus the products of the reaction are retarding the reaction rate.

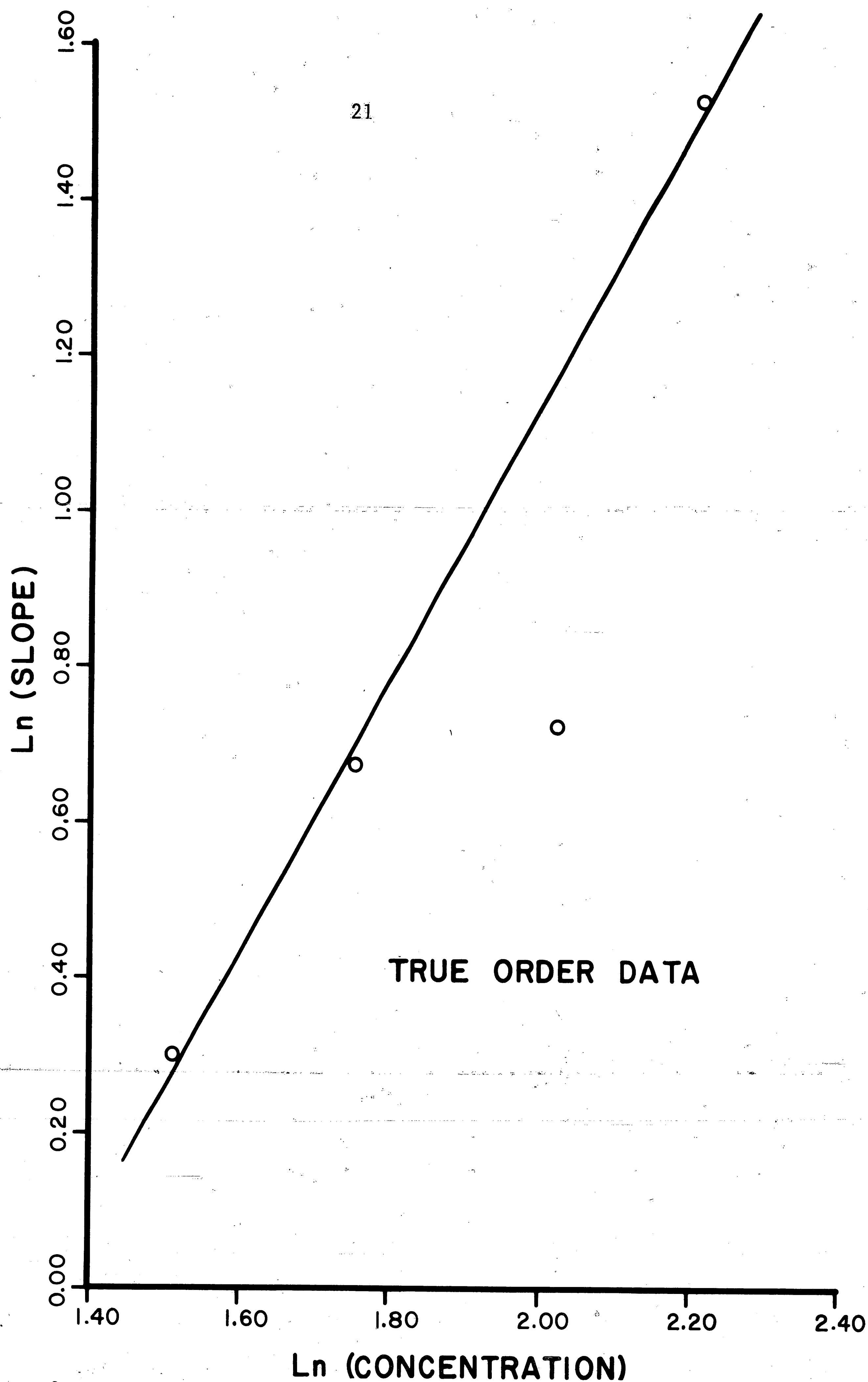


FIGURE 8: Data Taken from all Four Runs Produced a True Differential Reaction Order of 1.77.

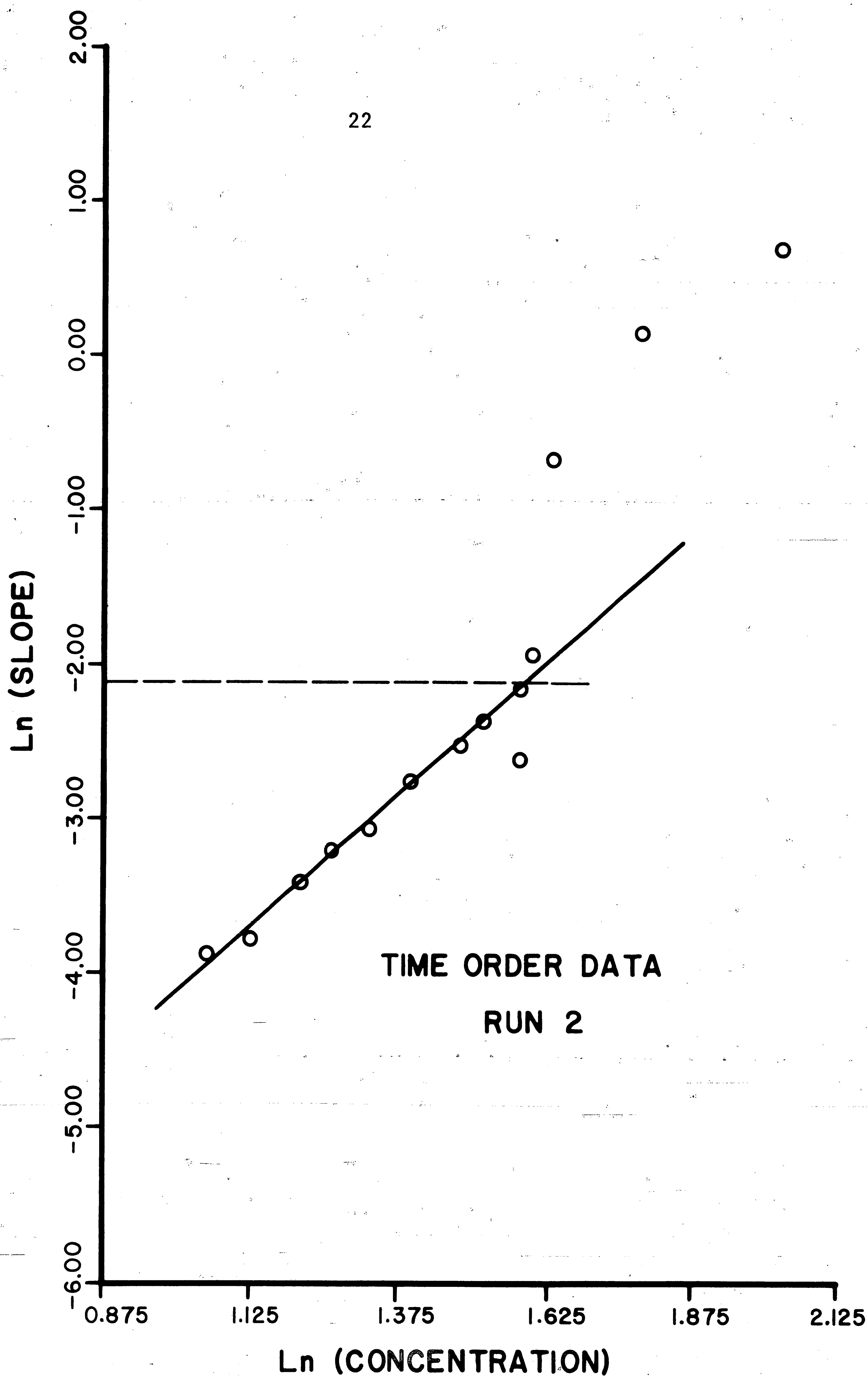


FIGURE 9: The Differential Time Order for Run 2 Was Found to be 3.38.

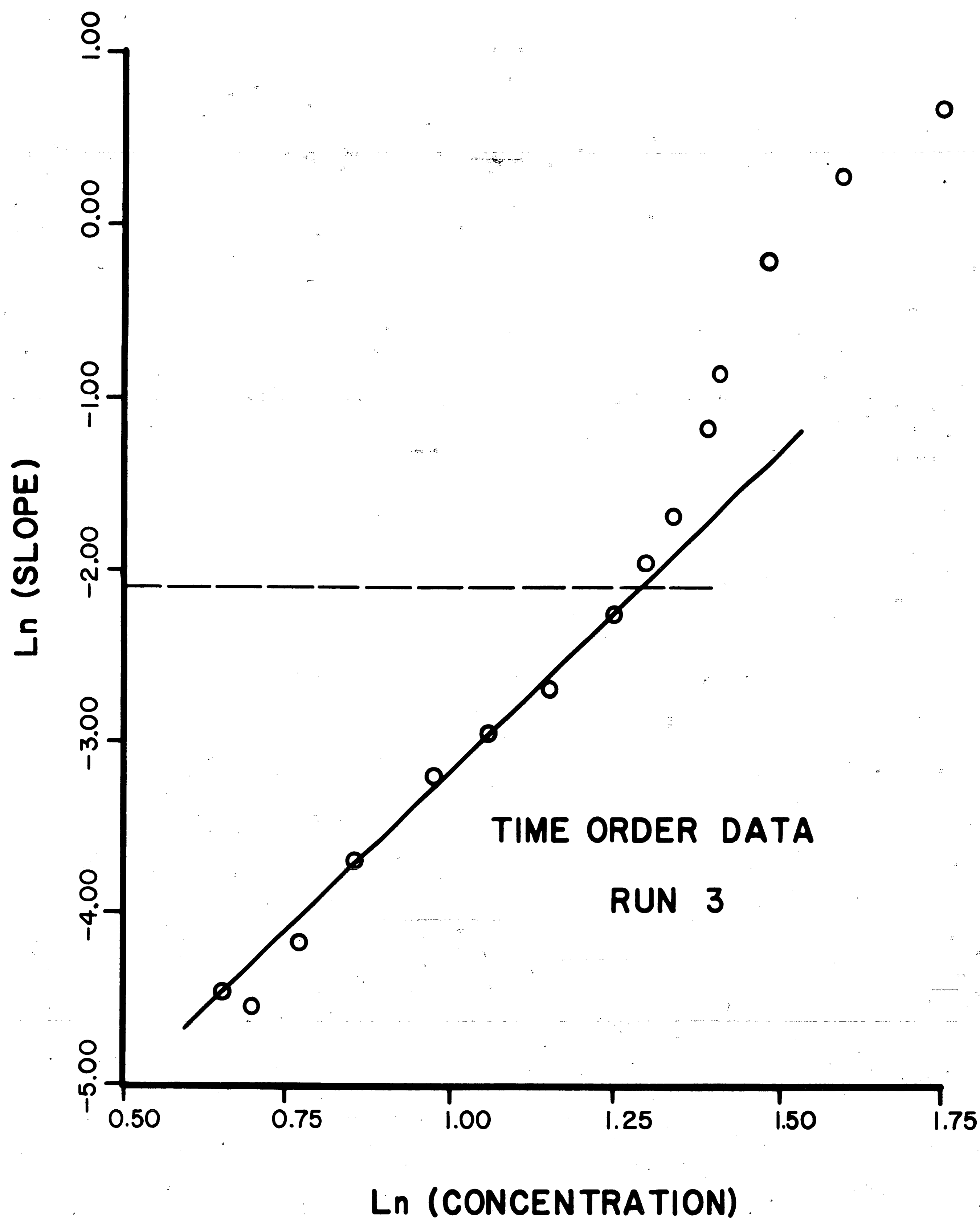


FIGURE 10: The Differential Time Order for Run 3 Was Found to be 3.72.

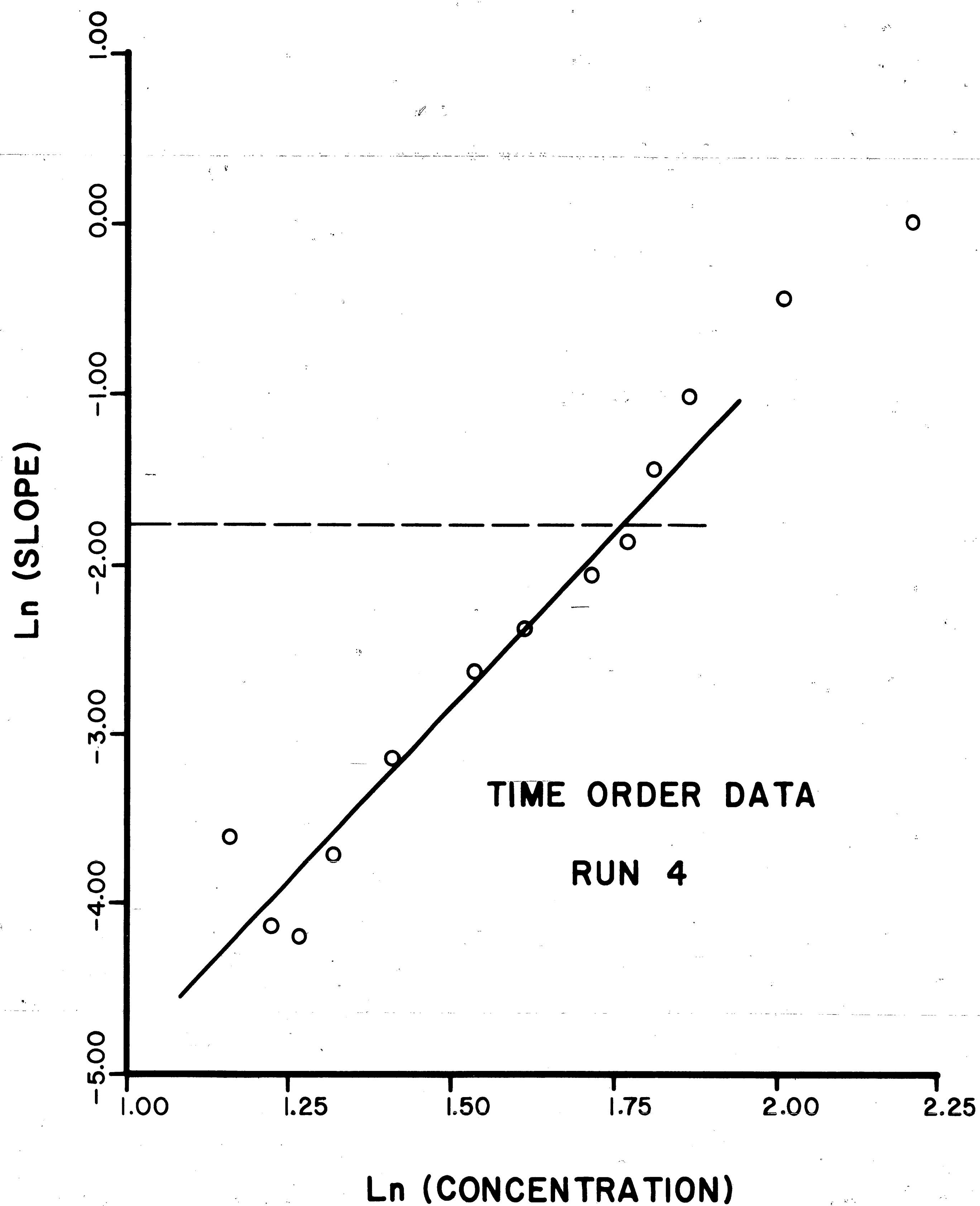


FIGURE 11: The Differential Time Order for Run 4 Was Found to be 4.06.

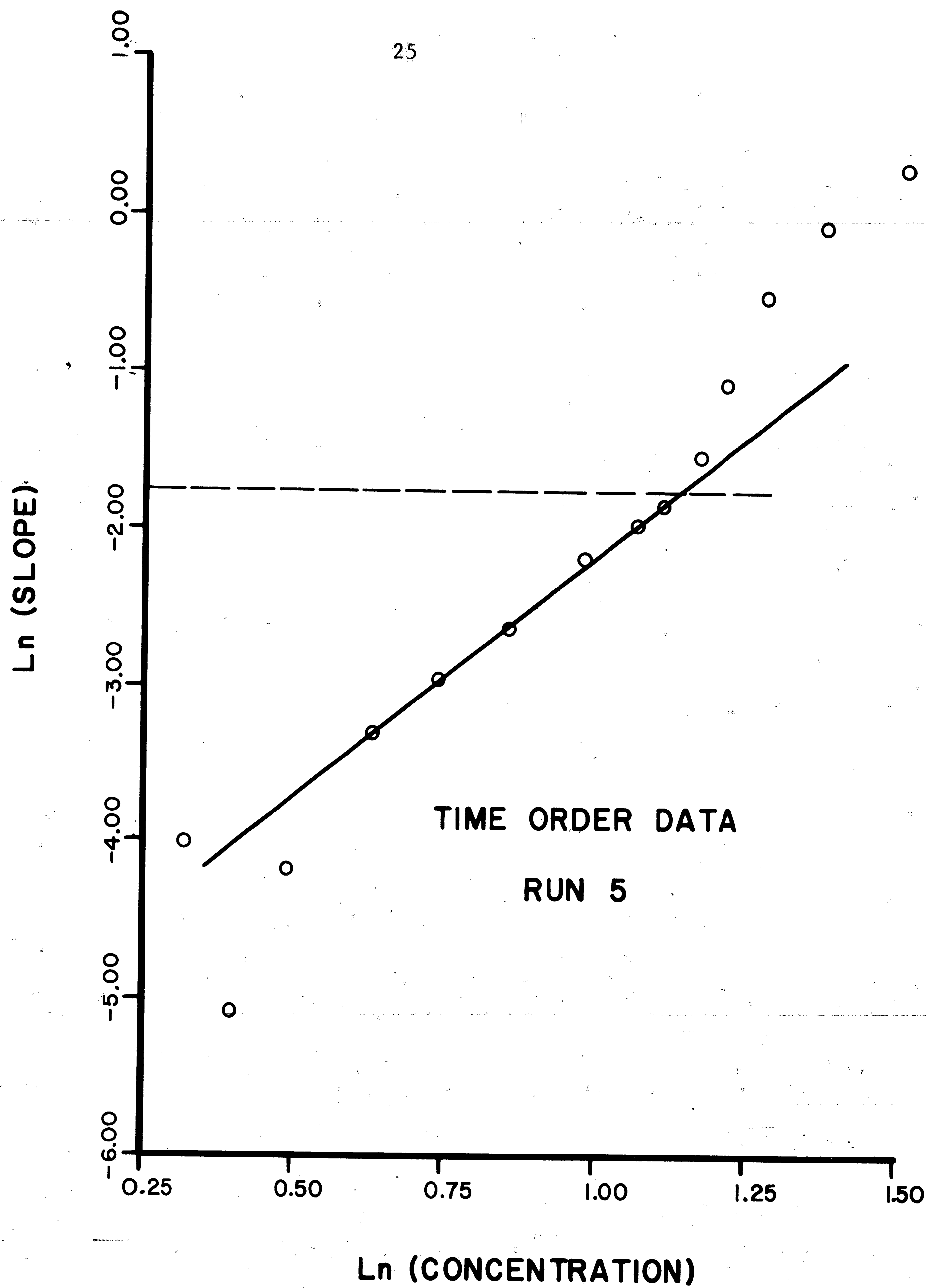


FIGURE 12: The Differential Time Order for Run 5 Was Found to be 3.05.

Mass Transfer Model

Szekely's mass transfer model was used as the next approach. As mentioned earlier, this approach was essentially a model of the open hearth furnace in which CO bubbles nucleated on the hearth floor rose up through the iron and slag. These bubbles, if there are enough of them, are very efficient in stirring the system. He assumed that the reaction was controlled by diffusion which could be described by the following equation (Appendix I):

$$C_i = \bar{C}_i + \operatorname{erfc} \left(\frac{z}{2\sqrt{D_i t}} \right) \quad (10)$$

Using the proper boundary conditions, Szekely derived an analytical expression for the flux of the species of interest. The equation for the flux appropriate for the system under study is as follows:

$$\bar{N}_{\text{MnO}} = \sqrt{\frac{D_{\text{MnO}}}{\pi t e}} \left[\alpha + (\alpha^2 + 4\beta)^{\frac{1}{2}} \right] \quad (11a)$$

$$\alpha = \sqrt{\frac{D_{\text{MnO}} D_{\text{C}}}{D_{\text{Mn}}}} \left[K\bar{C}_{\text{CO}} + \bar{C}_{\text{MnO}} \sqrt{\frac{D_{\text{Mn}}}{D_{\text{C}}}} - \bar{C}_{\text{C}} \sqrt{\frac{D_{\text{Mn}}}{D_{\text{MnO}}}} \right] \quad (11b)$$

$$\beta = \left(\sqrt{\frac{D_{\text{MnO}} D_{\text{C}}}{D_{\text{Mn}}}} \right) \left[\bar{C}_{\text{MnO}} \bar{C}_{\text{C}} - K\bar{C}_{\text{CO}} \bar{C}_{\text{Mn}} \right] \quad (11c)$$

The equations were derived for the reaction given by equation 1.

Since the flux was derived for conditions of constant bulk concentration and diffusivity, data from Run 5 were treated as individual cases and the observed flux was compared against the flux calculated by the model. The results are shown in Table V. Observed

fluxes were obtained through the slopes to the concentration vs. time curve (calculated by least squares) and a constant slag-metal interfacial area was assumed. Considering that a constant value of the diffusivity of the MnO in the slag had to be assumed, the results in Table V show good agreement.

The first results of the data without any further discussion show that the reaction has an initial order of around two. A consistent time order was not found for the second stage of the reaction, but time orders varying from 3.05 to 4.06, depending on the initial slag concentration, were found. It can be said that the products of the reaction interfere with the reaction rate from a comparison of the true and time orders. The reaction could also be broken into two stages by the time order differential data. The first stage consisted of a region with an initial order of about two which degenerated into a second stage with a reaction order of from three to four. Finally, it was found that a mass transfer model such as Szekely's could predict the observed reaction rates.

DISCUSSION

First Stage

In the first few minutes of the reaction, a reversible second-order kinetic expression appeared to fit the data for each of all four runs. A true differential order of 1.77 was found using data from all four runs. Considering the accuracy involved in measuring the true initial order, the initial order of the reaction is considered to be second order with respect to MnO in the slag. It should be noted that this stage involves considerable slag agitation (visually observed) due to gas evolution and a large range of initial MnO concentrations in the slag was employed.

An argument for chemical reaction control can be qualitatively stated in the absence of more exhaustive data. The transport or diffusion path should be extremely small in the slag due to the gas induced agitation. The extent to which the metal was agitated was not known; however, pieces and bubbles of iron were found in the slag samples. Therefore, the effect of diffusion in the iron and slag in this stage should be small. Another indication of a chemical mechanism is the absence of any influence of concentration and/or physical properties of the slag on the reaction kinetics. All of this supports the earlier hypothesis that, if the rate of stirring is increased to some point where diffusion is no longer important, then the rate of the chemical transfer of the species between the slag and the metal should be the important step in the overall reaction. The difference in rate behavior between the first and second stages seems to bear this idea out.

Second Stage

The reaction orders in the second stage vary with concentration in contrast to the concentration independent second-order kinetics of

the first stage of the reaction. Also, from the discrepancy between the differential true order and the differential time reaction orders, it is known that the products of the reaction are inhibiting the reaction rate. It would appear then that the rate is affected by factors influenced by slag composition and physical properties. Tarby and Philbrook also found an influence of composition on the activation energy of the process.

A mass transport-type argument may best describe the observed data. It does not seem unreasonable to expect the diffusion coefficients of the various species in the slag to vary with slag composition. Although little is known about diffusion in slags, it is known that changing the concentration of MnO in the slag will affect the slag viscosity.¹³ Theory of diffusion in liquids tells us that the diffusivity of a species in a liquid is inversely proportional to the viscosity of the liquid.¹⁴ Therefore, it should not be unreasonable to expect the reaction kinetics to change with the initial MnO concentration. It was found that larger values of D_{MnO} would increase the numerical value of the reaction order through use of the mass transfer model. The mass transfer model can therefore explain the change in time reaction orders with concentration. The mass transport concept should also explain the observed variation in the activation energies by considering that different slags (with different physical properties) should have different activation energies for diffusion.

The available data cannot give much information on which component is the slowest diffusing species. One could argue that, since the slag composition had such an important effect on the reaction, components dissolved in the slag are most important. On the other hand, it is probably true that the metal was not as thoroughly stirred as the slag and hence those species dissolved in the metal are the slowest moving. And then perhaps there is no one species moving appreciably slower than the rest. An educated guess would be that diffusion of

manganese in the metal away from the slag-metal interface or nucleation of CO bubbles is the rate limiting step since it is known that the products of the reaction are retarding the reaction rate.

The reaction can now be pictured as occurring in two stages. In the first stage, the overall reaction is probably controlled by an interfacial chemical reaction in the very first few minutes. Then as the reaction proceeds and the rate of gas induced stirring subsides, the reaction passes through a transition region of mixed control into the second stage (around 10-15 minutes after the start of the reaction) which is transport controlled. Throughout the reaction, the rate of the reaction exerts an effect on itself through the stirring mechanism. Szekely's model is capable of handling this effect and showing that a change in the diffusivity of MnO results in a change in the reaction rate (due both to increased reaction rate and increased stirring rate) and hence a change in the reaction order. Therefore, it is felt that this reaction indeed exhibits the transition of chemical to transport control predicted in the introduction.

CONCLUSIONS

The results of the investigation are summarized as follows:

1. The reaction may be divided into two stages.
2. The first stage of the reaction spans the period from the start of the reaction to the time (approximately 10-15 minutes) when a differential time order for the reaction appears. This stage has a reaction order of approximately two for the first four to eight minutes. It is felt that the reaction is chemically controlled during these four to eight minutes and then it enters a transition region between chemical and transport control.
3. The second stage starts at the time when a differential time reaction order may be determined. This stage is controlled by the transport of products and/or reactants.
4. The difference between the differential true and time orders indicate that the products of the reaction are retarding the reaction rate.

TABLE I

MATERIALS USED IN PROJECT

<u>Material</u>	<u>Source</u>	<u>Grade</u>	<u>Purity %</u>
CaCO_3	J. T. Baker	Reagent	99.6
SiO_2	Fisher		
Al_2O_3	J. T. Baker	Reagent	99.3
MnO_2	J. T. Baker	Reagent	99.9
Crucibles	Ultra Carbon	Spectrographic	4 ppm
CO gas	Air Products		99.5
Fe	Glidden	Electrolytic	99.9

TABLE II

EXPERIMENTAL DATA SLAG ANALYSIS

RUN 2

<u>Time (Min)</u>	<u>Wt. Pct. Mn</u>	<u>Wt. Pct. Fe⁺⁺</u>
0.0	7.75	
1.0	5.51	
2.0	5.18	
3.0	5.16	
4.0	4.97	
5.0	4.82	
7.5	4.53	
10.0	4.40	
15.0	4.04	
20.0	3.72	
25.0	3.53	
26.0		0.30
30.0	3.39	
40.0	3.03	
50.0	2.86	
59.0		0.21

TABLE II (Continued)

RUN 3

<u>Time (Min)</u>	<u>Wt. Pct. Mn</u>	<u>Wt. Pct. Fe++</u>
0.0	5.84	
0.5	4.77	
1.0	4.35	
1.5	4.21	
2.0	4.04	
3.0	3.80	
4.25	3.64	
6.0	3.51	
10.0	3.16	
15.0	2.86	
20.0	2.70	
25.0		0.31
30.0	2.34	
40.0	2.16	
52.0	2.01	
60.0	1.92	
60.5		0.24

TABLE II (Continued)

RUN 4

<u>Time (Min)</u>	<u>Wt. Pct. Mn</u>
0.0	9.26
2.0	7.06
4.0	6.45
5.167	6.34
7.5	5.89
10.0	5.47
15.0	5.08
20.0	4.60
30.0	4.10
40.0	3.71
50.0	3.56
60.0	3.38
70.0	3.19

TABLE II (Continued)

RUN 5

<u>Time (Min)</u>	<u>Wt. Pct. Mn</u>
0.0	4.64
0.5	3.80
1.0	3.62
1.5	3.42
2.5	3.27
3.583	3.03
4.583	2.87
6.5	2.71
10.167	2.34
15.0	2.09
20.0	1.92
30.0	1.63
40.0	1.60
50.0	1.48
60.0	1.38

TABLE III

INTEGRAL SECOND ORDER DATA

RUN 2

<u>Time (Min)</u>	<u>Wt. Pct. Mn</u>	<u>2nd Order Expression</u>	<u>k_1/K</u>
0.0	5.51	0.0000	
1.0	5.18	0.00742	2.64
2.0	5.16	0.00790	1.40
3.0	4.97	0.01265	1.50
4.0	4.82	0.01666	1.48
6.5	4.53	0.02515	1.38
9.0	4.40	0.02937	1.16

RUN 3

0.0	4.77	0.0000	
0.5	4.35	0.00889	0.731
1.0	4.21	0.01224	0.510
1.5	4.04	0.01663	0.457
2.5	3.80	0.02350	0.387
3.75	3.64	0.02858	0.314
5.5	3.51	0.03305	0.248
9.5	3.16	0.04691	0.203

TABLE III (Continued)

RUN 4

<u>Time (Min)</u>	<u>Wt. Pct. Mn</u>	<u>2nd Order Expression</u>	<u>k_1/K</u>
0.0	7.06	0.0000	
2.0	6.45	0.00954	1.32
3.167	6.34	0.01145	1.01
5.5	5.89	0.02003	1.01
8.0	5.47	0.02931	1.01
13.0	5.08	0.03931	0.84

RUN 5

0.0	3.80	0.0000	
0.5	3.62	0.00458	4.72
1.0	3.42	0.01023	5.28
2.0	3.27	0.01492	3.85
3.083	3.03	0.02339	3.91
4.083	2.87	0.02983	3.78
6.0	2.71	0.03703	3.18
9.667	2.34	0.05745	3.06

TABLE IV

TIME ORDERS OF THE EXPERIMENTAL RUNS

<u>Run</u>	<u>Initial Mn Concentration in the Slag (Wt. Pct.)</u>	<u>Differential Time Order</u>
5	4.64	3.05
3	5.84	3.72
2	7.75	3.38
4	9.26	4.06

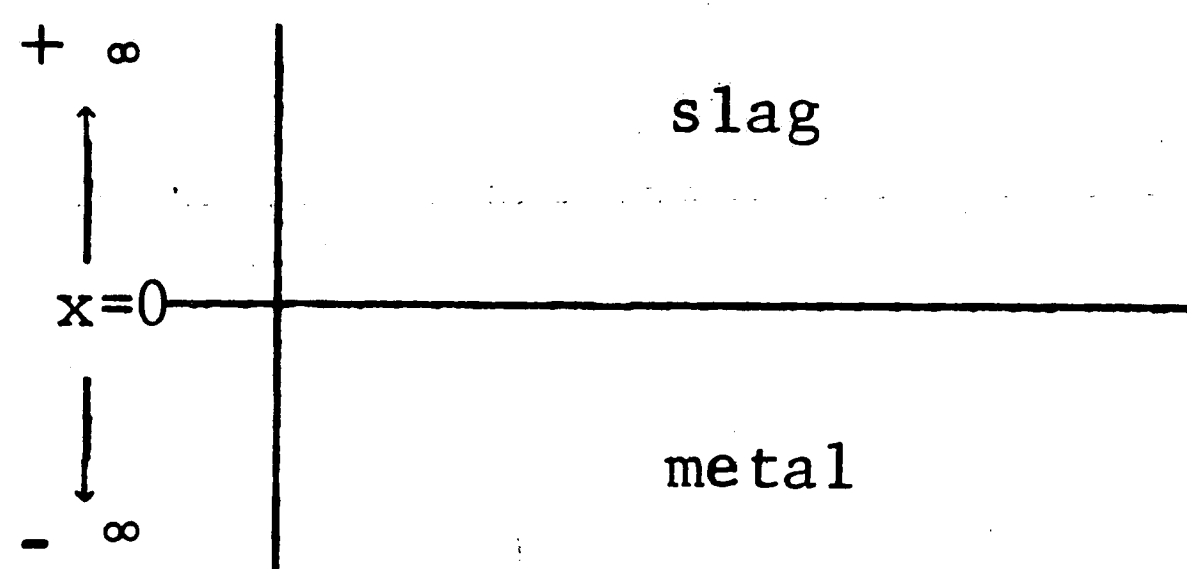
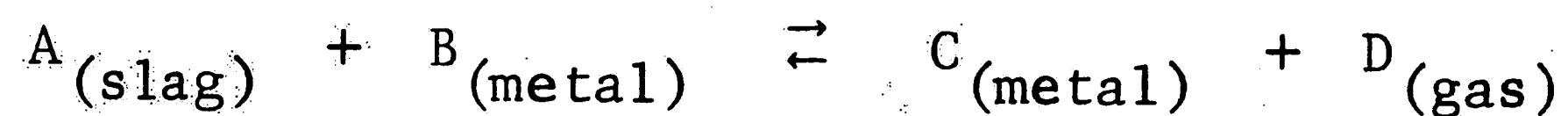
TABLE V

COMPARISON OF FLUXES PREDICTED BY
SZEKELY'S MODEL WITH THE OBSERVED FLUXES

<u>Time (Min)</u>	<u>Wt. Pct. Mn in Slag</u>	<u>Observed Flux Moles/(cm²-Min)</u>	<u>Calculated Flux Moles/(cm²-Min)</u>
0.0	4.64	9.77×10^{-4}	1.08×10^{-3}
0.5	3.80	6.76×10^{-4}	7.30×10^{-4}
1.0	3.62	4.32×10^{-4}	5.55×10^{-4}
1.5	3.42	2.46×10^{-4}	3.94×10^{-4}
2.5	3.27	1.55×10^{-4}	2.99×10^{-4}
3.583	3.03	1.13×10^{-4}	2.36×10^{-4}
4.583	2.87	1.01×10^{-4}	2.10×10^{-4}
6.50	2.71	8.07×10^{-5}	1.77×10^{-4}
10.167	2.34	5.21×10^{-5}	1.22×10^{-4}
15.0	2.09	3.76×10^{-5}	9.19×10^{-5}
20.0	1.92	2.67×10^{-5}	7.07×10^{-5}
30.0	1.63	1.12×10^{-5}	3.84×10^{-5}
50.0	1.48	4.48×10^{-6}	2.18×10^{-5}
60.0	1.38	1.38×10^{-6}	3.48×10^{-5}

APPENDIX I

The following instantaneous reaction is assumed to take place at the slag-metal interface.



For the following differential equation and boundary conditions, the following solution has been assumed^{7,12}:

$$D_i \frac{\partial^2 C_i}{\partial x_i^2} = \frac{\partial C_i}{\partial t} \quad (1)$$

where D_i = diffusivity of species i

C_i = molar concentration of species i

t = time

\bar{C}_i = bulk concentration

The boundary conditions for Eq. 1 are:

$$C_i = \bar{C}_i \quad \text{at } t = 0 \quad (2a)$$

$$C_i \rightarrow \bar{C}_i \quad \text{at } x \rightarrow +\infty \quad (2b)$$

$$\text{solution: } C_i = \bar{C}_i + A_i \operatorname{erfc} \frac{x}{2\sqrt{D_i t}} \quad (3)$$

The following conditions are assumed for the above reaction:

$$\frac{C_A C_B}{C_D C_C} = K \quad \text{at } x = 0 \quad (4)$$

$$D_A \frac{\partial C_A}{\partial x} = - D_B \frac{\partial C_B}{\partial x} = + D_C \frac{\partial C_C}{\partial x} \quad \text{at } x = 0 \quad (5)$$

(Species D is not included in the above expression since it is a gas.)

Substitution of Eq. 3 into Eq. 4 gives:

$$\frac{(\bar{C}_A + A_A)(\bar{C}_B + A_B)}{(\bar{C}_C + A_C)(\bar{C}_O)} = K \quad (\text{at } x = 0) \quad (6)$$

Differentiating Eq. 3 for the flux, one gets for Eq. 5:

$$\frac{2}{\sqrt{\pi}} \frac{D_A A_A}{2\sqrt{D_A t}} \exp - \frac{x^2}{2\sqrt{D_A t}} = \dots$$

Setting $x = 0$ simplifies the above equation:

$$A_A \sqrt{D_A} = - A_B \sqrt{D_B} = A_C \sqrt{D_C} \quad (7)$$

Substitution of Eq. 7 in Eq. 6 yields:

$$\frac{(\bar{C}_A + A_C \sqrt{\frac{D_C}{D_A}})(\bar{C}_B - A_C \sqrt{\frac{D_C}{D_B}})}{(\bar{C}_C + A_C) \bar{C}_O} = K \quad (8)$$

Expanding Eq. 8 yields:

$$\bar{C}_A \bar{C}_B + A_C \left[\bar{C}_B \sqrt{\frac{D_C}{D_A}} - \bar{C}_A \sqrt{\frac{D_C}{D_B}} \right] - A_C^2 \frac{D_C}{\sqrt{D_A D_B}} = K \bar{C}_C \bar{C}_D + K A_C \bar{C}_D \quad (9)$$

$$-A_C^2 \left(\frac{D_C}{\sqrt{D_A D_B}} \right) + A_C \left(\bar{C}_B \sqrt{\frac{D_C}{D_A}} - \bar{C}_A \sqrt{\frac{D_C}{D_B}} - K \bar{C}_D \right) + \bar{C}_A \bar{C}_B - K \bar{C}_C \bar{C}_D = 0 \quad (10)$$

Solving Eq. 10 by the quadratic formula yields:

$$A_C = \frac{- \left(\bar{C}_B \sqrt{\frac{D_C}{D_A}} - \bar{C}_A \sqrt{\frac{D_C}{D_B}} - K \bar{C}_D \right) \pm \sqrt{\left(\bar{C}_B \sqrt{\frac{D_C}{D_A}} - \bar{C}_A \sqrt{\frac{D_C}{D_B}} - K \bar{C}_D \right)^2 + 4 \frac{D_C}{\sqrt{D_A D_B}} (\bar{C}_A \bar{C}_B - K \bar{C}_C \bar{C}_D)}}{2 \frac{D_C}{\sqrt{D_A D_B}}}$$

$$A_C = \frac{1}{2} \left\{ \frac{\sqrt{D_A D_B}}{D_C} \left(K \bar{C}_D + \bar{C}_A \sqrt{\frac{D_C}{D_B}} - \bar{C}_B \sqrt{\frac{D_C}{D_A}} \right) \pm \left[\left(\bar{C}_B \sqrt{\frac{D_C}{D_A}} - \bar{C}_A \sqrt{\frac{D_C}{D_B}} - K \bar{C}_D \right)^2 + \frac{4 \sqrt{D_A D_B}}{D_C} (\bar{C}_A \bar{C}_B - K \bar{C}_C \bar{C}_D) \right]^{\frac{1}{2}} \right\} \quad (11)$$

$$\alpha = \frac{\sqrt{D_A D_B}}{D_C} \left(K \bar{C}_D + \bar{C}_A \sqrt{\frac{D_C}{D_B}} - \bar{C}_B \sqrt{\frac{D_C}{D_A}} \right) \quad (11a)$$

$$\beta = \frac{\sqrt{D_A D_B}}{D_C} \left(\bar{C}_A \bar{C}_B - K \bar{C}_C \bar{C}_D \right) \quad (11b)$$

$$\therefore C_C = \bar{C}_C + \frac{1}{2} \left[\alpha \pm \sqrt{\alpha^2 + 4\beta} \right] \operatorname{erfc} \left(\frac{x}{2\sqrt{D_C t}} \right) \quad (12)$$

$$N_C(t) = D_C \frac{\partial C_C}{\partial t} \quad (\text{instantaneous flux}) \quad (13)$$

Differentiating Eq. 12 and substituting into Eq. 13 yields:

$$N_C(t) = D_C \left[-\frac{2}{\sqrt{\pi}} \frac{1}{2} \frac{A_C}{2\sqrt{D_C t}} \exp - \left(\frac{x}{2\sqrt{D_C t}} \right)^2 \right] = -\frac{A_C}{2} \sqrt{\frac{D_C}{\pi t}} \quad \text{at } x = 0 \quad (14)$$

$$\bar{N}_C = \frac{1}{te} \int_0^{te} N_C(t) dt \quad (15)$$

The average flux is the average of the instantaneous fluxes over the period between successive rising bubbles.

$$\bar{N}_C = \frac{1}{te} \int_0^{te} -\frac{A_C}{2} \sqrt{\frac{D_C}{\pi t}} dt = -\frac{A_C}{2te} \sqrt{\frac{D_C}{\pi}} \int_0^{te} \frac{dt}{\sqrt{t}} \quad (16)$$

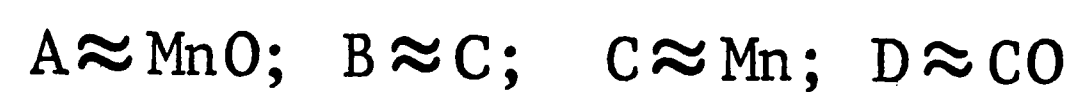
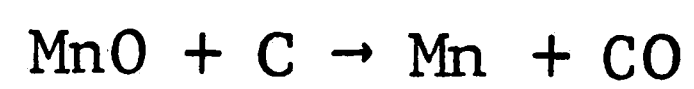
Using Eq. 5 at $x = 0$, the following relation between A_A and A_C may be obtained:

$$A_A = A_C \sqrt{\frac{D_C}{D_A}} \quad (17)$$

$$\therefore N_A(t) = D_A^{1/2} \sqrt{\frac{D_C}{D_A}} [\alpha \pm (\alpha^2 + 4\beta)^{1/2}] \left[-\frac{2}{\sqrt{\pi}} \frac{1}{2\sqrt{D_A t}} \exp - \left(\frac{x}{2\sqrt{D_A t}} \right)^2 \right] = \frac{\sqrt{D_C}}{2} [\alpha \pm (\alpha^2 + 4\beta)^{1/2}] \frac{1}{\sqrt{\pi t}} \quad (18)$$

Since Eq. 18 and 14 are the same, the flux can be written as:

$$\bar{N}_A = -\sqrt{\frac{D_C}{\pi t e}} [\alpha \pm (\alpha^2 + 4\beta)^{1/2}] \quad (19)$$



SAMPLE CALCULATIONS

$$C_{\text{MnO}} = \frac{(\text{MnO}^{\text{w/o}})(\text{slag wt})}{100 (\text{M.W.}_{\text{MnO}})} \times \frac{(\text{slag density})}{(\text{slag wt})}$$

$$C_{\text{MnO}} \left| \begin{array}{l} \text{at} \\ \text{equilibrium} \end{array} \right. = \frac{(0.165\%)(151.0\text{g})}{(100)(70.9)} \times \frac{(2.79 \text{ g/cm}^3)}{(151\text{g})} =$$

$$6.50 \times 10^{-5} \frac{\text{mole}}{\text{cm}^3}$$

$$C_{\text{Mn}} \left| \begin{array}{l} \text{at} \\ \text{equilibrium} \end{array} \right. = 1.38 \times 10^{-3} \frac{\text{mole}}{\text{cm}^3}$$

(The Mn-MnO equilibrium values were determined from W. O. Philbrook and S. K. Tarby: Trans TMS-AIME, 1963, Vol. 227, pp. 1039.)

$$C_{\text{C}} \left| \begin{array}{l} \text{at} \\ \text{equilibrium} \end{array} \right. = 2.94 \times 10^{-2} \frac{\text{mole}}{\text{cm}^3}$$

$$C_{\text{CO}} \left| \begin{array}{l} \text{at} \\ \text{equilibrium} \end{array} \right. = \frac{(273^\circ\text{K})}{(1773^\circ\text{K})(22,400 \frac{\text{cm}^3}{\text{mole}})} = 6.90 \times 10^{-6} \frac{\text{mole}}{\text{cm}^3}$$

$$K = \frac{C_{\text{MnO}} \cdot C_{\text{C}}}{C_{\text{Mn}} \cdot C_{\text{CO}}} = \frac{(6.50 \times 10^{-5})(2.94 \times 10^{-2})}{(1.38 \times 10^{-3})(6.90 \times 10^{-6})} = 2.01 \times 10^2$$

$$\text{bubble rate} = \frac{(\text{Mn}^{\text{w/o}}/\text{min})(\text{slag wt})}{100(54.9 \frac{\text{g}}{\text{mole}})} \times \frac{(22400 \frac{\text{cm}^3}{\text{mole}}) 1773^\circ\text{K}}{(273^\circ\text{K})(\text{bubble vol})}$$

$$\text{bubble vol} = \frac{4}{3} \pi r^3 = \frac{4}{3} \pi \left(\frac{2.54 \text{ cm/in}}{64 \text{ 1/in}} \right)^3 = 2.62 \times 10^{-4} \text{ cm}^3$$

$$\text{bubble cross sectional area} = \pi \left(\frac{2.54}{64} \right)^2 = 4.95 \times 10^{-3} \text{ cm}^2$$

$$\text{bath cross sectional area} = \pi [(1.375)(2.54)]^2 = 38.0 \text{ cm}^2$$

te = time between successive rising bubbles =

$$\frac{(\text{bath x-s area})}{(\text{bubble rate})(\text{bubble x-s area})} = \frac{7.68 \times 10^3}{\text{bubble rate}}$$

At 6.5 minutes into Run 5:

$$D_{\text{MnO}} = 6 \times 10^{-5} \text{ cm}^2/\text{min}$$

$$D_{\text{C}} = 1.77 \times 10^{-2} \text{ cm}^2/\text{min}$$

$$D_{\text{Mn}} = 5.04 \times 10^{-3} \text{ cm}^2/\text{min}$$

$$\alpha = \frac{[(6.0 \times 10^{-5})(1.77 \times 10^{-2})]^{\frac{1}{2}}}{(5.04 \times 10^{-3})} [(201.0)(6.90 \times 10^{-6}) - (2.94 \times 10^{-2})$$

$$\left(\frac{5.04 \times 10^{-3}}{6.0 \times 10^{-5}} \right)^{\frac{1}{2}} + (1.38 \times 10^{-3}) \left(\frac{5.04 \times 10^{-3}}{1.77 \times 10^{-2}} \right)^{\frac{1}{2}}] =$$

$$5.452 \times 10^{-2}$$

$$\beta = \frac{[(6.0 \times 10^{-5})(1.77 \times 10^{-2})]^{\frac{1}{2}}}{(5.04 \times 10^{-3})} [(1.38 \times 10^{-3})(2.94 \times 10^{-2}) -$$

$$(201.0)(6.9 \times 10^{-6})(6.11 \times 10^{-4})] = 8.115 \times 10^{-6}$$

$$A = 2.969 \times 10^{-4}$$

$$\bar{N}_{\text{MnO}} = A \sqrt{\frac{D_{\text{Mn}}}{\pi t e}} = 2.969 \times 10^{-4} \left[\frac{5.04 \times 10^{-3}}{\pi(1.70 \times 10^6)} \right]^{\frac{1}{2}} = 1.77 \times 10^{-4} \frac{\text{moles}}{\text{cm}^2 \text{ min}}$$

The observed flux is $8.07 \times 10^{-5} \frac{\text{moles}}{\text{cm}^2 \text{ min}}$

APPENDIX II

CHEMICAL ANALYSIS PROCEDURE OF SLAGS FOR MANGANESE

1. Crush sample to -100 mesh and then magnetically clean the sample (without water).
2. Weigh sample into a 600 ml beaker. Most sample weights were between one and two grams.
3. Dissolve the sample in 30-60 ml boiling 1:1 HCL and 5 ml HNO_3 .
4. Add 20 ml 1:1 H_2SO_4 after the sample has completely dissolved and fume down to approximately 20 ml volume twice. (HF acid was used in amounts just sufficient to dissolve any silicates.)
5. Dilute beaker contents to approximately 100 ml and slowly reheat to dissolve CaSO_4 .
6. Cool beaker and bring to volume in a 250 ml volumetric flask and allow precipitate to settle out.
7. Aliquot an amount equivalent to 5 mg Mn into a 500 ml erlynmeyer flask.
8. Add 20 ml mixed acids (100 ml H_2SO_4 , 125 ml H_3PO_4 , 250 ml HNO_3 , and 525 ml H_2O) and 10 ml of AgNO_3 solution (8g/100 ml) and bring flask to approximately 150 ml and then boil.
9. Add 10 ml of ammonium persulfate solution (250 g/1000 ml) and boil for 75 seconds.

10. Cool flask to room temperature and titrate with sodium arsenite solution (0.05%). (The arsenite solution is standardized against a known slag sample using the above procedure.)

APPENDIX III

DERIVATION OF THE REVERSIBLE INTEGRAL SECOND ORDER EXPRESSION

The following equation was assumed:



Writing the rate equation produces:

$$\frac{dC_A}{dt} = k_1 C_A^2 - k_2 C_R^2 \quad (2)$$

If $C_{R_0} = 0$:

$$C_A = C_{A_0} (1 - X_A) \quad \text{and} \quad C_R = C_{A_0} X_A$$

The equilibrium expression may be written as follows:

$$K_C = \frac{k_1}{k_2} = \frac{C_{A_0}^2 (X_{A_e})^2}{C_{A_0}^2 (1 - X_{A_e})^2} = \frac{X_{A_e}^2}{(1 - X_{A_e})^2} \quad (3)$$

The rate expression is now rewritten in terms of X_A :

$$C_{A_0} \frac{dX_A}{dt} = k_1 C_{A_0}^2 (1 - X_A)^2 - k_2 C_{A_0}^2 X_A^2 \quad (4)$$

$$\int_0^{X_A} \frac{dX_A}{k_1 - 2k_1 X_A + (k_1 - k_2) X_A^2} = \int_0^t C_{A_0} dt \quad (5)$$

The solution to this integral is of the following form:

$$\int \frac{dx}{a + bx + Cx^2} = \frac{1}{\sqrt{b^2 - 4ac}} \ln \frac{2cx + b - \sqrt{b^2 - 4ac}}{2cx + b + \sqrt{b^2 - 4ac}} \quad (6)$$

$$\sqrt{b^2 - 4ac} = \sqrt{4k_1^2 - 4k_1(k_1 - k_2)} = 2\sqrt{k_1 k_2} = 2k_1 \sqrt{\frac{k_2}{k_1}} \quad (7)$$

Equation 3 is used to eliminate k_2 producing:

$$2k_1 \sqrt{\frac{k_2}{k_1}} = \frac{2k_1}{\sqrt{K_C}} \quad (8)$$

Equation 3 may also be used to simplify Eq. 6:

$$\ln \left\{ \frac{1 - \left[\frac{(1-X_A)_e^2}{X_{Ae}^2} \right] X_A - 1 - \left[\frac{1-X_A}{X_A} \right] \left[-1 + \left(\frac{1-X_A}{X_A} \right) \right]}{1 - \left[\frac{(1-X_A)_e^2}{X_{Ae}^2} \right] X_A - 1 + \left[\frac{1-X_A}{X_A} \right] \left[-1 + \left(\frac{1-X_A}{X_A} \right) \right]} \right\} =$$

$$\frac{2k_1}{\sqrt{K_C}} C_{A0} t \quad (9)$$

The final form of the solution is given by Eq. 10:

$$\ln \left\{ \frac{X_{Ae} - (2X_{Ae} - 1) X_A}{(X_{Ae} - X_A)} \right\} = \frac{2k_1}{\sqrt{K_C}} C_{A0} t \quad (10)$$

APPENDIX IV

DERIVATION OF DIFFERENTIAL RELATIONS

$$\text{Rate} = -\frac{1}{s} \frac{dn}{dt} = k C_{\text{MnO}}^x \quad (1)$$

The above rate equation describes the kinetics for the reaction under study. It is implicitly assumed that the carbon concentration is constant and part of the rate constant, and the reaction is irreversible. However, the equation as written is not in its most useful form.

$$-\frac{1}{s} \frac{dn}{dt} = -\frac{1}{s} \frac{d}{dt} \left[\frac{(\text{Wt. Pct. Mn})(\text{Wt. Slag})}{(\text{M.W. of Mn})} \right] = k \left[\frac{(\text{Wt. Pct. Mn})(\text{Wt. Slag})}{(\text{M.W. of Mn})(\text{Slag Volume})} \right]^x \quad (2)$$

$$-\frac{(\text{Wt. Slag})}{s(\text{M.W. of Mn})} \frac{d(\text{Wt. Pct. Mn})}{dt} = \frac{k(\text{Wt. Slag})^x}{(\text{M.W. of Mn})^x (\text{Slag Volume})^x} (\text{Wt. Pct. Mn})^x \quad (3)$$

If the slag-metal interfacial area is considered constant, the above equation may be further simplified:

$$-C_1 \frac{d(\text{Wt. Pct. Mn})}{dt} = k C_2^x (\text{Wt. Pct. Mn})^x \quad (4)$$

Taking the logarithm of Eq. 4:

$$\ln - C_1 + \ln \left[\frac{d(\text{Wt. Pct. Mn})}{dt} \right] = \ln (k C_2^x) + x \ln (\text{Wt. Pct. Mn}) \quad (5)$$

$$\ln \left[\frac{d(\text{Wt. Pct. Mn})}{dt} \right] = \ln(\text{rate}) = C_3 + x \ln(\text{Wt. Pct. Mn}) \quad (6)$$

(C_1, C_2, C_3 are constants)

Equation 6 is now in a form suitable for plotting. The slope of the curve, x , will correspond to the order of the reaction with respect to MnO .

REFERENCES

1. F. D. Richardson: Iron and Coal, Nov. 24, 1961, pp. 1105-1116.
2. S. K. Tarby and W. O. Philbrook: Trans TMS-AIME, 1967, Vol. 239, pp. 1005-1017.
3. D. M. Koncsics: Masters Thesis, Lehigh University, Bethlehem, Pennsylvania, 1968.
4. F. Fun: Met. Trans., 1970, Vol. 1, pp. 2537-2541.
5. K. J. Laidler: Chemical Kinetics, 2nd edit., Chap. 1, McGraw-Hill, New York, 1965.
6. A. W. D. Hills: Heterogeneous Kinetics at Elevated Temperatures, Belton and Worrell ed., pp. 449-501, Plenum Press, New York, 1970.
7. L. S. Darken and E. T. Turkdogan: op. cit., pp. 25-99.
8. P. V. Danckwerts: Ind. and Eng. Chem., 1951, Vol. 43, pp. 1460-1467.
9. E. T. Turkdogan, P. Grieveson, and J. F. Beisler: Trans TMS-AIME, 1963, Vol. 227, pp. 1265-1274.
10. W. L. Daines and R. D. Pehlke: Trans TMS-AIME, 1968, Vol. 242, pp. 565-575.
11. J. Szekely: Int. J. Heat and Mass Transfer, 1963, Vol. 6, pp. 1077-1082.
12. F. W. Ruch: Private Communication.
13. M. Kato and S. Minowa: Trans ISIJ, 1969, Vol. 9, pp. 31-38.
14. R. Bird, W. Stewart, and E. Lightfoot: Transport Phenomena, Chap. 16, John Wiley and Sons, New York, 1966.

VITA

Charles Kendall Clarke was born on April 11, 1945, in Ray, Arizona. His parents are Mr. and Mrs. Otis Manson Clarke. He graduated from Tuscaloosa Senior High School, Tuscaloosa, Alabama, in 1963 and then entered the University of Alabama. He received a Bachelor of Science degree in Metallurgical Engineering in January 1968 and attended one semester of graduate school at Alabama. In July 1968, Mr. Clarke entered the Graduate School at Lehigh University to study in the Department of Metallurgy and Materials Science.

He is married to the former Carolyn Faye Daniels of Bay Minette, Alabama.